Biodesign

pISSN 2288-6982 | eISSN 2288-7105

CRYSTALLIZATION P 49-52

Expression, crystallization, and preliminary X-ray crystallographic analysis of peptide deformylase from *Acinetobacter baumanii*

Thien-Hoang Ho[1,+], Kyoungho Jung[1,+], Inho Lee[1], Kim-Hung Huynh[1], Diem-Quynh Nguyen[1], Hyunjae Park[1], Sang Hee Lee[2] and Lin-Woo Kang[1,*]

[1]Department of Biological Sciences, Konkuk University, 120 Neungdong-ro, Gwangjin-gu, Seoul 05029, Korea, [2]National Leading Research Laboratory of Drug Resistance Proteomics, Department of Biological Sciences, Myongji University, 116 Myongjiro, Yongin, Gyeonggido 17058, Korea. *Correspondence: lkang@konkuk.ac.kr

[+]These authors contribute equally for this paper.

The emergences of multi-drug resistant bacteria such as *Acinetobacter baumanni* have emphasized the necessity of new antibiotics. Peptidyl deformylase (PDF) catalyzes the removal of the formyl group from the N-terminal formylated methionine residue present in all nascent polypeptides in bacteria. In this study, the PDF gene from *Acinetobacter baumannii* K0420859 was cloned and its protein was overexpressed in *E. coli*, purified, and crystallized. The purified protein was crystallized using the hanging-drop vapour-diffusion method and the crystal diffracted to 2.4 Å resolution. The crystal belonged to the trigonal space group $P3_2$ with unit cell parameters of $a = b = 39.4$ Å and $c = 187.9$ Å. Two protomers were presented in the asymmetric unit with a corresponding V_M of 2.10 Å^3 Da^{-1} and a solvent content of 41.5%.

INTRODUCTION

Acinetobacter baumannii is a Gram-negative round- or rod-shaped bacterium. In hospital outbreaks, *Acinetobacter baumannii* is one of the most important nosocomial pathogens causing bacteremia, pneumonia, and other repiratory and urinary tract infections (Antunes et al., 2011; Espinal et al., 2013; Mosqueda et al., 2013).

Peptide deformylase (PDF) is essential for bacteria survival. Bacterial protein synsthesis begins with a *N*-formylmethionine, which is formed from methionyl-tRNA by *N*-methionyl-tRNA transformylase (Lin et al., 2010). N-formylmethionine is frequently removed from the nascent protein (Waller, 1963). In the first step of the process, PDF removes the *N*-formyl group from newly synthesized polypeptide chain. Consequently, methionine aminopeptidase (MAP) removes the N-terminal methionine (Ngo et al., 2008; Miesel et al., 2003). The inhibition of PDF activity results in the disruption of protein maturation or processing and causes the bacterial cell death (Chang et al., 1989; Miller et al., 1989). Although PDF is essential in bacteria, mammalian PDF is nonessential. Currently, PDF is considered as a potential target for the antibacterial drug development.

Thus far, crystal structures of bacterial PDFs in complex with inhibitors have been determined from *Streptococcus pneumoniae* (Axten et al., 2012), *Streptococcus agalactiae* (Fieulaine et al., 2016), *E. coli* (Clements et al., 2001), *Streptococcus aureus* (Lee et al., 2012), and *Xanthomonas oryzae* pv. oryzae (Ngo et al., 2016). For example, actinonin, a naturally occurring hydroxamate pseudotripeptide from *Streptomyces* Cutter C/2, is a potent inhibitor of bacterial PDFs and an antibacterial agent (Chen et al., 2000). Most of the inhibitors bind in the substrate-binding pocket of PDFs as actinonin.

Enzymatic properties of currently characterized bacteria PDFs are similar and their overall structures are well conserved in spite of low sequence homology among them. However, even a point mutation on target protein can cause a drastic change in the affinity of drugs. *PDF* genes are ubiquitous in bacteria. We were interested in the structural and functional studies of bacterial PDFs. The three-dimensional structural study will be useful for the development of new antibacterial drugs against PDFs. In this study, we cloned the *PDF* gene from *Acinetobacter baumannii* K0420859 (*AbPdf*) and expressed its protein in *E. coli*. We also purified, crystallized its protein, and performed a preliminary X-ray crystallographic study of AbPdf crystal.

RESULTS AND DISCUSSION

The purification protocol for the recombinant form of AbPdf consistently yielded more than 5 mg of AbPdf per liter of culture medium and the protein exhibited a single band on SDS-PAGE at approximately 21 kDa (Figure 1). Crystals were obtained by mixing 0.5 µl of protein solution with 0.5 µl of reservoir solution, which contained 0.03 M $MgCl_2$, 0.03 *M* $CaCl_2$, 15% (*v*/*v*) PEGMME, 15% (*w*/*v*) PEG 20000, 0.1 *M* Tris (base)/ Bicine pH 8.5. After two weeks, crystals grew to maximum dimensions of approximately 0.005 x 0.12 x 0.005 mm (Figure 2). X-ray diffraction data were collected at the beamline 5C SB II of PLS in Republic of Korea. The space group was selected using the

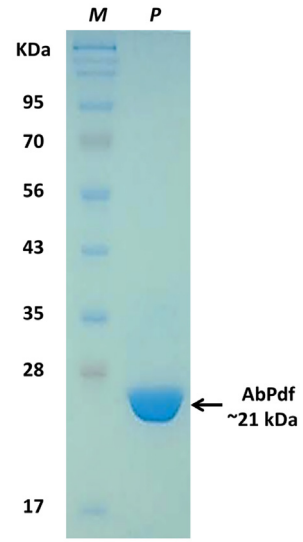

FIGURE 1 | Purified AbPdf on a 12% SDS-PAGE gel. Molecular-mass markers are shown in lane *M* and purified AbPdf is shown in lane *P*.

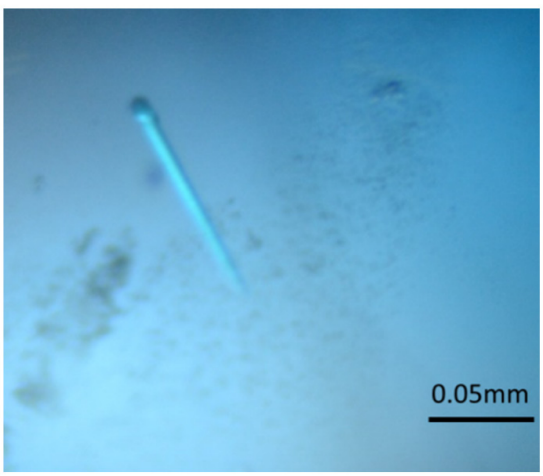

FIGURE 2 | Crystal of AbPdf. Initial crystals were obtained in two weeks using a reservoir solution containing 0.03 *M* $MgCl_2$, 0.03 *M* $CaCl_2$, 15% (*v*/*v*) PEGMME, 15% (*w*/*v*) PEG 20000, and 0.1 *M* Tris (base)/Bicine pH 8.5 from MD1-46 (Morpheus™). The scale bar represents 0.05 mm.

auto-indexing program in *HKL-2000* (Zbyszek Otwinowski, 1997) and data-collection statistics are provided in Table 1. The AbPdf crystal belonged to the crystallographic space group $P3_2$, with unit-cell parameters of $a = b = 39.4$ Å and $c = 187.9$ Å. According to calculation of the Mathews coefficient (Mathews, 1968), two molecules were presented in the asymmetric unit, with a corresponding V_M of 2.10 $Å^3\ Da^{-1}$ and a solvent content of 41.5%. Molecular replacement using *MOLREP* (Vagin and Teplyakov, 2010) from the *CCP4* program package (Winn et al., 2011) with PDF from *Staphylococcus aureus* (PDB entry 1S17 (Molteni et al., 2004) and sequence identity 68.3%) as a

TABLE 1 | Data-collection and processing statistics

X-ray source	Beamline 5C SB II, PLS
Wavelength (Å)	0.97960
Detector	ADSC Q315r
Crystal-to-detector distance (mm)	300
Rotation range per image (°)	1
Total rotation range (°)	316
Exposure time per image (s)	3
Resolution range (Å)	50.0-2.4 (2.44-2.40)
Space group	$P3_2$
Unit-cell parameters (Å, °)	$a = b$ =39.4, c = 187.9
	$\alpha = \beta$ = 90.0, γ = 120.0
Mosaicity (°)	0.3
Total No. of reflections	48,799
No. of unique reflections	12,427
Redundancy	3.9 (4.5)
Mean $I/\sigma(I)$	30.0 (5.9)
Completeness (%)	96.9 (100.0)
$R_{p.i.m}$† (%)	5.7 (23.8)
No. of molecules in the asymmetric unit	2
Solvent contents (%)	41.5
V_M ($Å^3\ Da^{-1}$)	2.10

†$R_{p.i.m} = \sum_{hkl}[1/(N-1)]^{1/2}\sum_i | I_i(hkl) - I(hkl) | / \sum_{hkl}\sum_i I_i(hkl)$ where $I_i(hkl)$ is the intensity of reflection *hkl*, $\sum_{hkl}$ is the sum over all reflections, and $\sum_i$ is the sum over i measurements of reflection *hkl*. Values in parentheses are for highest-resolution shell.

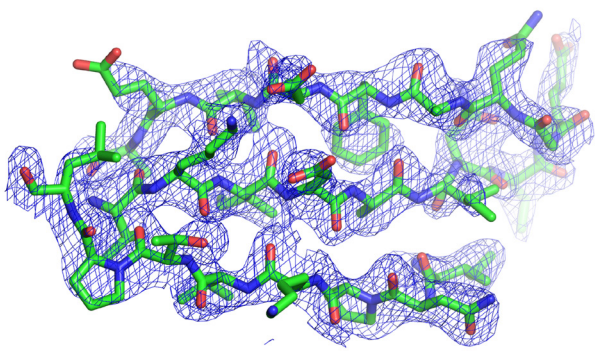

FIGURE 3 | Initial 2Fo-Fc maps of AbPdf structure. The 2Fo-Fc maps (contoured at 1.0 σ) are shown as blue meshes.

search model was successful and showed two protomers in the asymmetric unit. After rigid body and first restrained refinement by Refmac5 (Murshudov et al., 2011), the values of R_{work} and R_{free} were 22.1 and 28.7%, respectively (Figure 3). The further refinement is being carried out. The structural details will be described in a separate paper.

METHODS

Cloning

The gene encoding the AbPdf protein was amplified by PCR using the genomic DNA isolated from *Acinetobacter baumannii* K0420859 as a template. The sequences of the oligonucleotide primers were designed based on the data on genome sequences of other *Acinetobacter baumannii* species from the NCBI website. Forward (5'- CCC CCC **CAT ATG** GCC TTA TTA CCT ATT TTA AG -3') and reverse (5'- CCC **GGA TCC** TTA ACG TTT TAC CGC AAC TTT TTC -3') primers were designed to introduce NdeI and BamHI restriction sites (bold), respectively. The PCR-amplified DNA fragments were purified using a PCR purification kit (Bioneer) and inserted into the same restriction enzyme digested pET11aHT vector, which was engineered to have additional residues of a 7×His tag and a Tobacco etch virus (TEV) protease-cleavage site before the NdeI site in the pET11a vector (Novagen). The expression vector pET11aHT-AbPdf was transformed into *E. coli* BL21(DE3), and plated on Luria-Bertani agar containing 50 μg ml^{-1} ampicillin. An ampicillin-resistant colony was selected and plasmid DNA from the transformant was isolated using a plasmid purification kit (Favorgen). DNA sequencing to confirm the cloning was carried out at the Macrogen facility (Seoul, Korea).

Overexpression and purification

E. coli BL21 (DE3) cells containing pET11aHT-*AbPdf* were grown at 310 K to OD_{600} of 0.6 in Luria-Bertani medium supplemented with 50 μg ml^{-1} ampicillin. The protein expression of AbPdf was induced by the addition of isopropyl β-D-1-thiogalactopyrasnoside (IPTG) to a final concentration of 0.5 m*M*. The cells were cultured at 310 K. After overnight growth, cells were then harvested by centrifuging at 6000 × g (Vision VS24-SMTi V5006A rotor) for 20 min at 277 K. The resultant cell pellets were resuspended in ice-cold lysis buffer (25 m*M* Tris-HCl, pH 7.5, 300 m*M* NaCl, 10 m*M* imidazole and 3 m*M* β-mercaptoethanol) and disrupted using a sonicator (Sonomasher). The crude cell extract was centrifuged for 30 min at 21000 × g (Vision VS24-SMTi V508A rotor) at 277 K to remove cell debris. The supernatant containing soluble AbPdf was applied onto Ni-NTA resin (Bio-rad) previously equilibrated with the lysis buffer. All protein purification steps were carried out at 277 K. The elution buffer containing 250 m*M* imidazole was used to elute the 7×His-tagged AbPdf. The eluate was dialyzed for 8h at 277 K againt dialysis buffer (25 m*M* Tris-HCl pH 7.5, 15 m*M* NaCl, and 3 m*M* β-mercaptoethanol). The His-tag was cleaved by TEV protease at 277 K in an overnight reaction. AbPdf was purified again using Ni-NTA resin (Bio-rad). Further purification was carried out on a HiTrap Q Anion-exchange column (GE Healthcare) equilibrated in buffer A (25 m*M* Tris-HCl, pH 7.5, 15 m*M* NaCl, and 3 m*M* β-mercaptoethanol). AbPdf was washed and eluted with a gradient of 0 to 100% buffer B (25 m*M* Tris-HCl, pH 7.5, 1 M NaCl, and 3 m*M* β-mercaptoethanol). The homogeneity of purified protein was checked via SDS-PAGE (Fig. 1). For crystallization, the protein solution was concentrated using Centrifugal Filters (Amicon ® Ultra-15, MWCO 10 kDa) to a final concentration of 4.5 mg ml^{-1} in a buffer consisting of 25 m*M* Tris-HCl, pH 7.5, 15 m*M* NaCl and 3 mM β-mercaptoethanol.

Crystallization and X-ray data collection

Initial crystallization screening was carried out at 287 K using the Hydra II e-drop automated pipetting system (Matrix) on a 96-Well Intelliplate (Art Robbins). Drops consisted of 0.5 μl protein solution (4.5 mg ml^{-1}) and 0.5 μl reservoir solution and were equilibrated against 50 μl reservoir solution at 287 K. The initial crystallization conditions tested were from the MD1-46 (Morpheus™), Wizard precipitant synergy (EMERALD-BIO) and Hampton research kits (Crystal screen cryolite, Crystal screen HT, Index HT and Salt RX HT). An initial hit for AbPdf appeared in the MD1-46 (Morpheus™) kit after two weeks with a precipitant solution consisting of 0.03 *M* $MgCl_2$, 0.03 *M* $CaCl_2$, 15% (*v*/*v*) PEG550MME, 15% (*w*/*v*) PEG 20000, 0.1 *M* Tris (base)/ Bicine pH 8.5. The fully grown crystals were flash-cooled at 100 K in liquid nitrogen with the cryoprotectant solution (0.03 M $MgCl_2$, 0.03 M $CaCl_2$, 15% (*v*/*v*) PEGMME, 15% (*w*/*v*) PEG 20000, 0.1 *M* Tris (base)/ Bicine pH 8.5, and 20%(v/v) glycerol).

X-ray data were collected at 100 K using the ADSC Q315r detector on beamline 5C of the Pohang Light Source (PLS), Republic of Korea. X-ray diffraction data to 2.4 Å resolution were collected for the AbPdf crystal. Diffraction data were collected from a single crystal with 1° oscillation per frame for a total of 316° at a 300 mm crystal-to-detector distance and with 3 sec exposure per frame. The raw data were processed and scaled using *DENZO* and *SCALEPACK*, respectively (Zbyszek Otwinowski, 1997).

ACKNOWLEDGEMENTS

We are grateful to staff members at the beamline 5C SB II of PLS, Republic of Korea. This work was carried out with the support of "Cooperative Research Program for Agriculture Science & Technology Development (Project No. PJ01127901)" Rural Development Administration, Republic of Korea and written as part of Konkuk University's research support program for its faculty on sabbatical leave in 2016.

AUTHOR INFORMATION

The authors declare no potential conflicts of interest.

Original Submission: Feb 22, 2017
Revised Version Received: Feb 26, 2017
Accepted: Feb 26, 2017

REFERENCES

Antunes, L.C.S., Imperi, F., Carattoli, A., and Visca, P. (2011). Deciphering the multifactorial nature of Acinetobacter baumannii pathogenicity. *PLoS One* **6**, e22674.

Axten, J.M., Medina, J.R., Blackledge, C.W., Duquenne, C., Grant, S.W., Bobko, M.A., Peng, T., Miller, W.H., Pinckney, T., Gallagher, T.F., Kulkarni, S., Lewandowski, T., Van Aller, G.S., Zonis, R., Ward, P., Campobasso, N. (2012). Acylprolinamides: a new class of peptide deformylase inhibitors with in vivo antibacterial activity. *Bioorg Med Chem Lett* **22**, 4028-4032.

Chang, S.Y., McGary, E.C., and Chang, S. (1989). Methionine aminopeptidase gene of Escherichia coli is essential for cell growth. *J Bacteriol* **171**, 4071-4072.

Chen, D.Z., Patel, D.V., Hackbarth, C.J., Wang, W., Dreyer, G., Young, D.C., Margolis, P.S., Wu, C., Ni, Z.J., Trias, J., White, R.J., and Yuan, Z. (2000). Actinonin, a naturally occurring antibacterial agent, is a potent deformylase inhibitor. *Biochemistry* **39**, 1256-1262.

Clements, J.M., Beckett, R.P., Brown, A., Catlin, G., Lobell, M., Palan, S., Thomas, W., Whittaker, M., Wood, S., Salama, S., Baker, P.J., Rodgers, H.F., Barynin, V., Rice, D.W., and Hunter, M.G. (2001). Antibiotic activity and characterization of BB-3497, a novel peptide deformylase inhibitor. *Antimicrob Agents Chemother* **45**, 563-570.

Espinal, P., Macia, M.D., Roca, I., Gato, E., Ruiz, E., Fernandez-Cuenca, F., Oliver, A., Rodriguez-Bano, J., Bou, G., Tomas, M., and Vila, J. (2013). First report of an OXA-23 carbapenemase-producing Acinetobacter baumannii clinical isolate related to Tn2006 in Spain. *Antimicrob Agents Chemother* **57**, 589-591.

Fieulaine, S., Alves de Sousa, R., Maigre, L., Hamiche, K., Alimi, M., Bolla, J.M., Taleb, A., Denis, A., Pages, J.M., Artaud, I., Meinnel, T., and Giglione, C. (2016). A unique peptide deformylase platform to rationally design and challenge novel active compounds. *Sci Rep* **6**, 35429.

Lee, S.J., Lee, S.J., Lee, S.K., Yoon, H.J., Lee, H.H., Kim, K.K., Lee, B.J., Lee, B.I., and Suh, S.W. (2012). Structures of Staphylococcus aureus peptide deformylase in complex with two classes of new inhibitors. *Acta Crystallogr D Biol Crystallogr* **68**, 784-793.

Lin, P., Hu, T., Hu, J., Yu, W., Han, C., Zhang, J., Qin, G., Yu, K., Gotz,

F., Shen, X., Jiang, H., and Qu, D. (2010). Characterization of peptide deformylase homologues from Staphylococcus epidermidis. *Microbiology* **156**, 3194-3202.

Mathews (1968). Solvent content of protein crystals. *J Mol Biol* **33**, 491-497.

Miesel, L., Greene, J., and Black, T.A. (2003). Genetic strategies for antibacterial drug discovery. *Nat Rev Genet* **4**, 442-456.

Miller, C.G., Kukral, A.M., Miller, J.L., and Movva, N.R. (1989). pepM is an essential gene in Salmonella typhimurium. *J Bacteriol* **171**, 5215-5217.

Molteni, V., He, X., Nabakka, J., Yang, K., Kreusch, A., Gordon, P., Bursulaya, B., Warner, I., Shin, T., Biorac, T., Ryder, N.S., Goldberg, R., Doughty, J., and He, Y. (2004). Identification of novel potent bicyclic peptide deformylase inhibitors. *Bioorg Med Chem Lett* **14**, 1477-1481.

Mosqueda, N., Espinal, P., Cosgaya, C., Viota, S., Plasensia, V., Alvarez-Lerma, F., Montero, M., Gomez, J., Horcajada, J.P., Vila, J., and Roca, I. (2013). Globally expanding carbapenemase finally appears in Spain: nosocomial outbreak of acinetobacter baumannii producing plasmid-encoded OXA-23 in Barcelona, Spain. *Antimicrob Agents Chemother* **57**, 5155-5157.

Murshudov, G.N., Skubak, P., Lebedev, A.A., Pannu, N.S., Steiner, R.A., Nicholls, R.A., Winn, M.D., Long, F., and Vagin, A.A. (2011). REFMAC5 for the refinement of macromolecular crystal structures. *Acta Crystallogr D Biol Crystallogr* **67**, 355-367.

Ngo, H.P., Ho, T.H., Lee, I., Tran, H.T., Sur, B., Kim, S., Kim, J.G., Ahn, Y.J., Cha, S.S., and Kang, L.W. (2016). Crystal Structures of Peptide Deformylase from Rice Pathogen Xanthomonas oryzae pv. oryzae in Complex with Substrate Peptides, Actinonin, and Fragment Chemical Compounds. *J Agric Food Chem* **64**, 7307-7314.

Ngo, P.T., Kim, J.K., Kim, H., Jung, J., Ahn, Y.J., Kim, J.G., Lee, B.M., and Kang, L.W. (2008). Expression, crystallization and preliminary X-ray crystallographic analysis of peptide deformylase from Xanthomonas oryzae pv. oryzae. *Acta Crystallogr Sect F Struct Biol Cryst Commun* **64**, 1031-1033.

Vagin, A., and Teplyakov, A. (2010). Molecular replacement with MOLREP. *Acta Crystallogr D Biol Crystallogr* **66**, 22-25.

Waller, J.P. (1963). The Nh2-Terminal Residues of the Proteins from Cell-Free Extracts of E. Coli. *J Mol Biol* **7**, 483-496.

Winn, M.D., Ballard, C.C., Cowtan, K.D., Dodson, E.J., Emsley, P., Evans, P.R., Keegan, R.M., Krissinel, E.B., Leslie, A.G., McCoy, A., McNicholas, S.J., Murshudov, G.N., Pannu, N.S., Potterton, E.A., Powell, H.R., et al. (2011). Overview of the CCP4 suite and current developments. *Acta Crystallogr D Biol Crystallogr* **67**, 235-242.

Zbyszek Otwinowski, W.M. (1997). Processing of X-ray diffraction data collected in oscillation mode *Methods Enzymol* **276**, 307-326.

